UDC 551.515.5:551.589.1:551.507.362.2:551.576(084.1)(66)"1968.323"

SOME REMARKS ON AFRICAN DISTURBANCES AND THEIR PROGRESS OVER THE TROPICAL ATLANTIC

TOBY N. CARLSON

National Hurricane Research Laboratory, ESSA, Miami, Fla.

ABSTRACT

A daily analysis of the 2,000- and 10,000-ft streamlines over West Africa was made for a 3½-mo period beginning in July 1968. With the aid of satellite photographs and auxiliary sea-level pressure data, a total of 33 synoptic scale wave perturbations were observed to move across West Africa and the tropical Atlantic Ocean during this period. Some general features of these disturbances are summarized, including facts on their origin, speed, intensity, distribution of sea-level pressure, appearance on the satellite photographs, and movement over the Atlantic Ocean. The effects of the large-scale circulation and the influence of sea-surface temperatures on the movement and intensity of disturbances are also discussed.

1. INTRODUCTION

During the past 2 yr, investigations by Simpson and others (1968, 1969), Frank (1969), and Carlson (1969) (the latter henceforth will be referred to as paper I) have probed into the origin and complete life cycle of Atlantic tropical disturbances. Their results underscore the fact that the majority of disturbances that cross the Antilles from the east during the summer months originate over Africa, while comparatively few form within the maritime portion of the intertropical convergence zone (ITC). A large number of disturbances are found to cross the African coast during the summer, and most of these can be tracked as far as the Caribbean. Initial investigations into the continuity of African disturbances and their development into Atlantic hurricanes have been made by Erickson (1963) and Arnold (1966). Although only a very few of these disturbances develop into Atlantic tropical storms and hurricanes, African disturbances apparently account for a significant percentage of mid-season (August and September) storms.

It is therefore important to investigate the disturbances in their earlier stages over Africa where a data network makes it possible to readily identify synoptic scale features of the flow pattern. Following the method described in paper I, in which wave disturbances and their attendant cloud distributions were tracked across West Africa, a set of daily analyses for this region were constructed for an extended period during the summer of 1968 (July 5 to October 18). These analyses consist of 2,000- and 10,000-ft streamline charts and selected sea-level pressure traces for the portion of tropical West Africa between longitudes 25° W. and 20° E. With the further aid of satellite photographs, the movement of synoptic scale wave perturbations across West Africa was readily discernible. It is our intention in this paper to outline some general features of African disturbances and to relate their movement and development to external influences in the environment.

2. SYNOPTIC DESCRIPTION OF THE DISTURBANCES OVER AFRICA

Selected examples of the 2,000- and 10,000-ft streamline analyses have been superimposed on their respective satellite photographs for display in figures 1A–C and 2A–C. The disturbances are labeled in the figures by an arrow, which signifies the mean longitude of the wave axis at 10,000 ft (the level at which the disturbances were most easily recognizable). The arrows are labeled according to the date on which the wave axis crossed the longitude of Dakar, 17° W.; disturbance 9/11 therefore is that perturbation whose 10,000-ft axis reached 17° W. on September 11. Table 1 is a catalog of the African disturbances; listed in the first column are the date and time of wave passage at longitude 17° W. The date and longitude at which the disturbance first became recognizable are listed in column 2.

Altogether, 33 such disturbances were observed during the 3½-mo period, a frequency of one wave every 3.2 days. A series of traveling waves are clearly evident in the sequence of analyses in figure 1, the disturbances broadly corresponding to areas of cloud enhancement. A few disturbances presented difficulties in analysis and in construction of a smooth track, either because they weakened to the point of unrecognizability or because minor side lobes present in a number of waves became temporarily large enough to confuse the analysis. Usually it was possible to track the main wave pocket and with the aid of hindsight smoothing to remove sudden jumps in speed.

The mean wavelength of the disturbances was about 1,300 mi over West Africa; it is apparent from the analyses that there was a considerable meridional extent to the waves as well. This is further illustrated in figure 3, which shows that systematic variations in sea-level pressure accompanying the series of the waves analyzed in figure 1 occurred almost simultaneously over the 700-mi-long chain of coastal stations, A–F. As was the usual situation, the largest pressure variations occurred in the northern part of the network. A striking illustration of this fact is displayed in figure 3C in which the upper wave axis is shown to be preceded by 3- to 4-mb pressure falls at station A, 2-mb pressure falls at C, and about 1-mb falls at F. The figures listed in column four of table 1 represent the magnitude of the pressure oscillation (at about 16° N.) which accompanied the passage of the wave across the

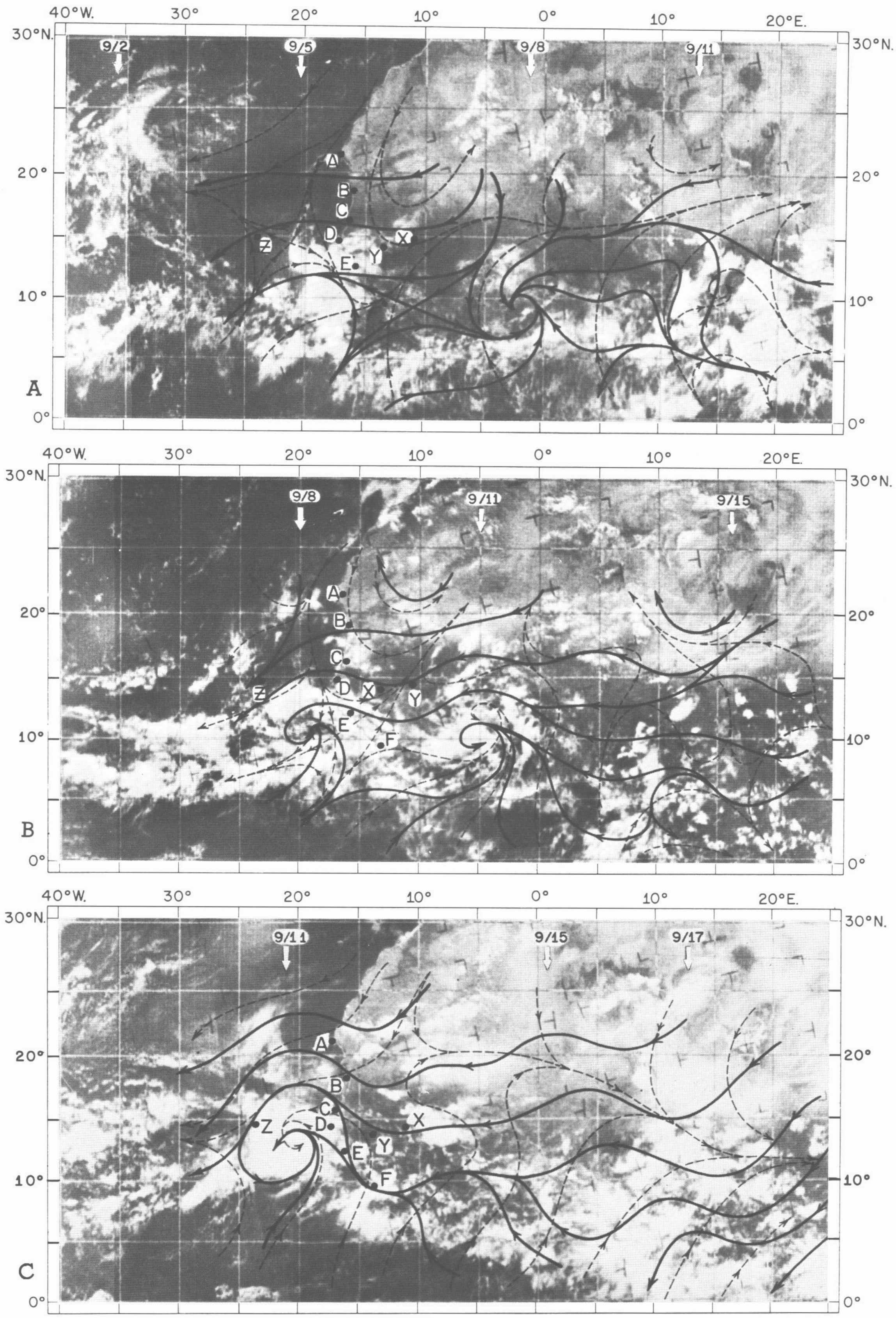

FIGURE 1.—A series of digitalized ESSA 7 satellite mosaics, upon which are superimposed the 10,000-ft (solid lines) and 2,000-ft (dashed lines) streamline analyses; (A) view at 1600 GMT on Sept. 5, 1968, and streamline analysis at 0000 GMT on Sept. 6, 1968; (B) view at 1600 GMT on Sept. 8, 1968, and streamline analysis at 0000 GMT on Sept. 9, 1968; (C) view at 1600 GMT on Sept. 11, 1968, and streamline analysis at 0000 GMT on Sept. 12, 1968. The capital letters shown in the vicinity of the West African coast refer to the location of the sea-level pressure barographs whose traces appear in figure 3. The longitudinal positions of the wave axis are indicated by an arrow and labeled according to the date the wave passed longitude 17° W.

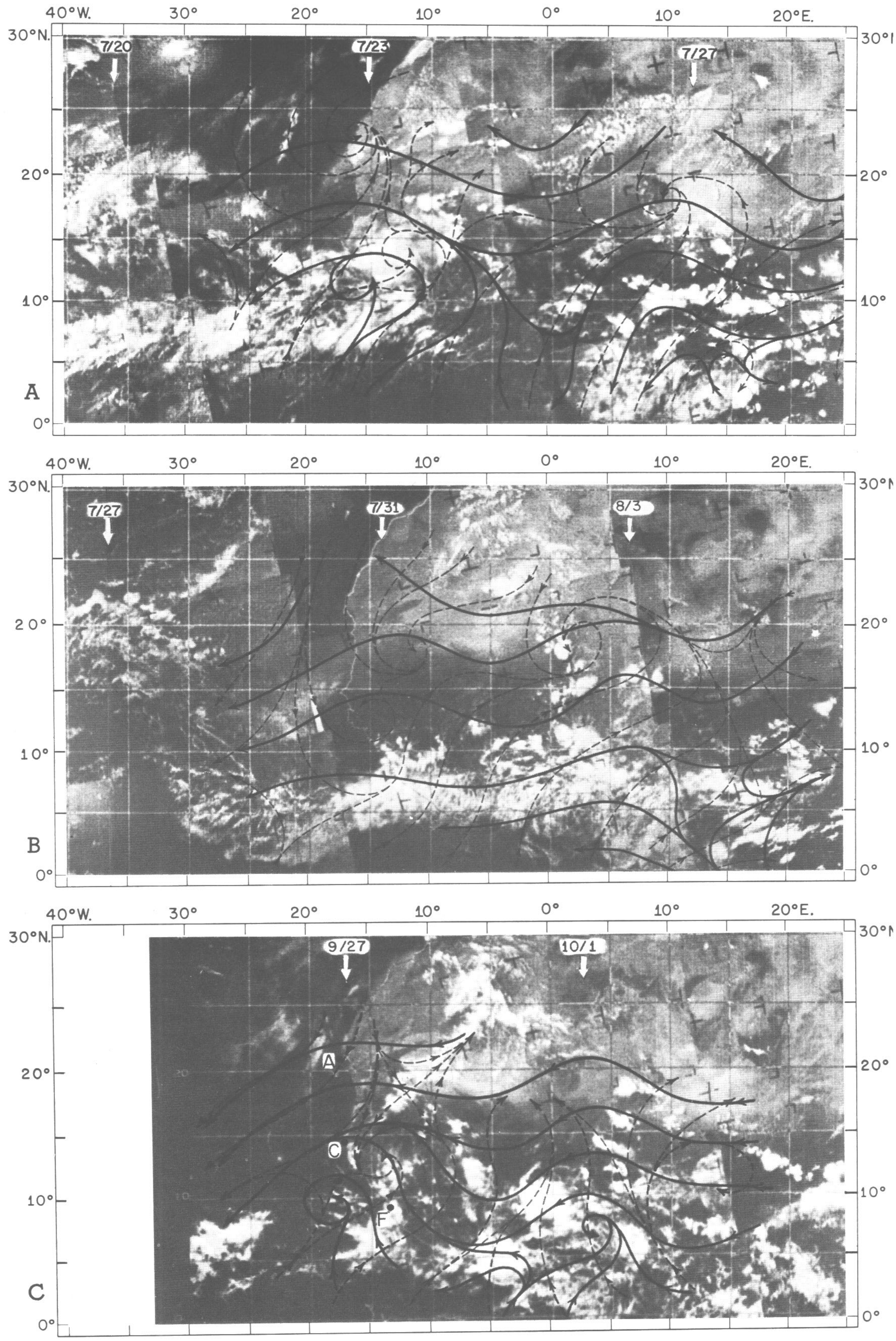

FIGURE 2.—Same as figure 1, but for selected examples of African disturbances; (A) view at 1600 GMT on July 22, 1968, and streamline analysis at 0000 GMT on July 23, 1968; (B) view at 1600 GMT on July 30, 1968, and streamline analysis at 0000 GMT on July 31, 1968; (C) view at 1600 GMT on Sept. 27, 1968, and streamline analysis at 0000 GMT on Sept. 28, 1968.

TABLE 1.—*African disturbances in 1968*

Wave Rchd. 17°W Mo/Day/Time (GMT)	Wave First Obsvd. Mo/Day/Long.	Speed Crossing W. Africa (kt)	Press. Fluc. 16°N, 17°W (mb)	Init. Location Surface Vortex, Other Details	Satellite Obs.: Init. Location Circular Cloud Pattern	Arrival 60°W Mo/Day	Speed Crossing At. Ocean (kt)	Last Obsvd. Mo/Day/Long.	Comments on Devel. West of Africa
07/07/0000		16.0	3.1		10°W, 12°N	07/13	18.0	07/16/82°W	
07/09/1800	7/08/07°W	22.0	2.5	Low Lat.		07/15	18.5	07/18/81°W	Wknd. 35°W
07/12/1200	07/08/15°E	17.5	4.1			07/18	19.5	07/24/94°W	
07/16/2100	07/11/23°E	20.0	3.0			07/22	17.5	07/27/93°W	
07/20/0600	07/15/11°E	14.5	2.4	05°W, 14°N	03°W, 14°N	07/26	19.0	07/28/68°W	
07/23/0900	07/18/19°E	16.0	2.7	07°W, 12°N	07°W, 12°N	07/29	16.0	08/04/86°W	
07/27/0600	07/22/19°E	16.5	2.7	18°W, 11°N	10°W, 12°N	08/03	16.0	08/07/78°W	
07/31/1200	07/25/10°E	12.5	5.0	05°W, 13°N	15°W, 12°N	08/07	17.0	08/11/80°W	Hurricane Dolly Florida Straits
08/03/1200	07/30/08°E	14.5	1.8	Low Lat. Weak 19°W, 11°N	13°W, 12°N	08/08	20.0	08/16/106°W	Tropical Storm in Pac. Ocean
08/06/1800	08/01/21°E	17.0	1.9	Notably Weak	14°W, 16°N	08/13	17.0	08/14/66°W	
08/09/0300	08/06/02°E	15.5	2.0	Notably Weak Low Lat.		08/15	17.5	08/20/91°W	
08/14/0000	08/05/21°E	10.5	2.7	16°W, 15°N	17°W, 12°N	08/20	18.5	08/23/79°W	
08/17/1200	08/13/12°E	16.5	4.8	21°W, 16°N	01°W, 11°N	08/23	18.5	08/26/82°W	Trop. Depression Gulf of Mexico Wknd. 50°W
08/20/1800	08/15/17°E	15.0	4.4	00°W, 11°N		08/28	14.0	09/02/82°W	Wknd. 34°W
08/24/1800	08/19/06°E	10.5	<1.0	Notably Weak Small Wave Length		09/01	13.0	09/07/92°W	Tropical Storm in Pac. Ocean
08/26/0600	08/21/10°E	13.0	1.8	Dominated by 08/28				08/30/38°W	
08/28/1800	08/21/20°E	15.0	4.5	13°W, 13°N	04°E, 14°N	09/05	15.0	09/06/64°W	Wknd. 32°W
09/02/1800	08/28/14°E	14.0	4.9	17°W, 13°N	02°W, 13°N	09/09	15.5	09/12/73°W	Wknd. 56°W
09/05/1200	08/31/20°E	16.5	2.8	Low Lat.	18°W, 12°N	09/12	16.0	09/17/87°W	
09/08/0600	09/04/06°E	13.0	3.5					09/15/58°W	Wknd. 35°W
09/11/0000	09/04/20°E	13.0	2.0	05°W, 13°N	05°W, 12°N	09/20	11.0	09/21/60°W	Hurricane Edna 37°W, 09/15 Wknd. 43°W
09/15/0000	09/08/18°E	13.0	2.9	12°W, 12°N		09/22	14.5	09/22/57°W	Wknd. 33°W
09/17/0900	09/11/19°E	14.5	3.3	17°W, 12°N Low Lat.		09/24	16.5	09/25/65°W	Wknd. 46°W
09/21/0000	09/16/12°E	12.0	3.5	13°W, 12°N		09/26	18.0	10/01/86°W	
09/22/2000	09/17/15°E	14.0	1.5	Low Lat. Weak		09/29	16.0	10/04/86°W	
09/27/1200	09/18/22°E	10.0	3.4	13°W, 12°N		10/05	14.5	10/07/70°W	Wknd. 33°W
10/01/0300	09/21/20°E	7.5	3.0	17°W, 14°N		10/09	11.5	10/10/65°W	Wknd. 37°W
10/03/1200	10/02/11°W	10.0	3.0	16°W, 13°N Part of 10/05?		10/12	13.5	10/13/65°W	Wknd. 41°W
10/06/0000	09/20/12°E	10.0	<1.0			10/14	13.0	10/16/67°W	
10/08/2100	10/05/03°E	13.0	3.9	03°W, 06°N Low Lat.		10/21	9.5	10/21/60°W	
10/13/0600	10/05/26°E	13.0	1.7	Low Lat. Weak				10/17/41°W	
10/14/0900	10/08/21°E	14.5	<1.0	Low Lat. Weak				10/17/26°W	
10/18/0000	10/11/19°E	12.5	3.3	12°W, 13°N		10/25	14.0	10/28/77°W	Wknd. 38°W

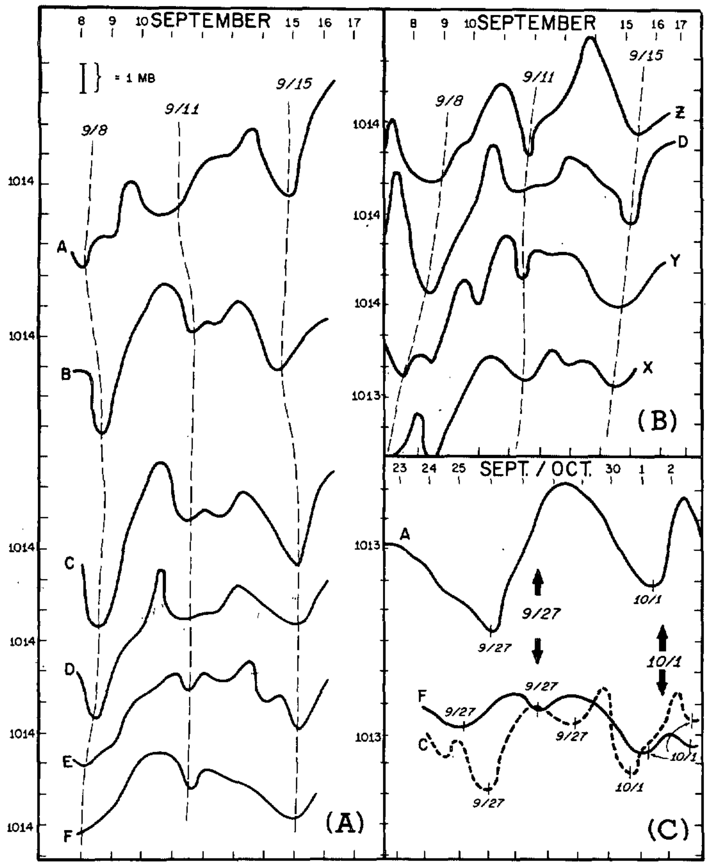

FIGURE 3.—(A) sea-level barograph traces (adjusted for diurnal trends) at the longitudinal sequence of stations A–F and (B) the latitudinal sequence of stations X–Z for the series of waves shown in figure 1; (C) the barograph traces for stations A, C, and F for a period beginning in late September.

network of coastal stations. Table 2 shows that the median value of this pressure fluctuation was close to 3.0 mb.

These large sea-level pressure fluctuations appear to be centered near 20° N. in the vicinity of a major cyclonic eddy which was often observed to move with the disturbances along the southern fringe of the desert in the confluence between moist air arriving from the south and dry Saharan air. An idealized representation of this vortex is shown in the schematic flow pattern of figure 4. The analyses in figures 2A–C contain examples of disturbances having attendant vortices located near latitude 20° N. which closely resemble the idealized analysis in figure 4. The lack of moisture associated with this vortex is apparent in the analyses which show that the latitude at which it is located is largely free of cloud, the main zone of cloudiness being centered far to the south. (The large fluctuations in sea-level pressure occurring at station A during the period September 23 to October 20 (fig. 3C) were unaccompanied by any rainfall or significant cumulus buildups.) According to figure 4 the mean areal cloud cover (an average of individual observations of cloud cover made from satellite photographs and determined with respect to the longitude of the wave axis for 23 disturbances in the vicinity of 10° W.) at 20° N. is generally less than 10 percent, although there is a slight increase noticeable in the amount of cover near the wave axis. It seems probable that the vortex located at this latitude is produced indirectly by the wave's circulation in which its formation is the result of a southward ad-

TABLE 2.—*Frequency distribution of sea-level pressure fluctuations accompanying wave passage at 17° W.*

Pressure interval (mb)	<1.0	1.0-1.9	2.0-2.9	3.0-3.9	4.0-4.9	≥5.0
Number of cases	3	5	9	10	5	1

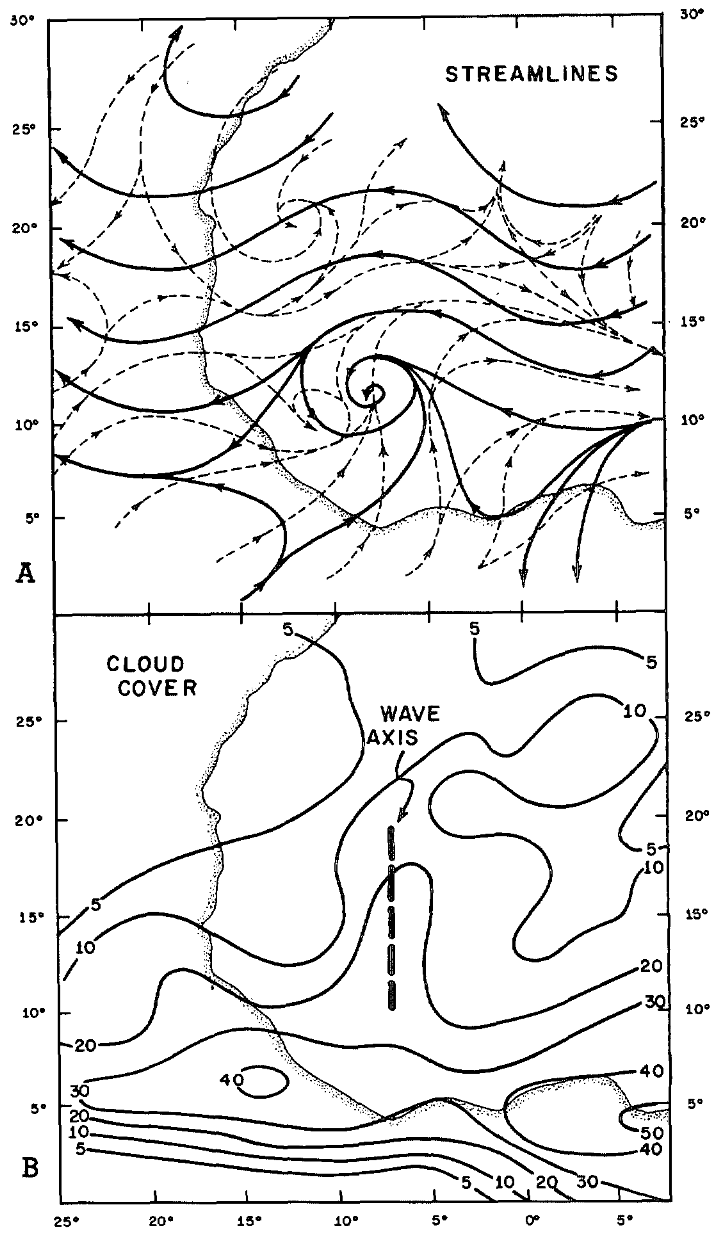

FIGURE 4.—(A) schematic flow pattern at 10,000 ft (solid lines) and 2,000 ft (dashed lines) for the typical African disturbance; (B) contours show a mean percentage cover of cloud with respect to the schematic flow pattern shown in (A). The field represents an average cover for 23 disturbances as measured near 10° W.

TABLE 3.—*Distance surface-pressure trough lies ahead (to the west) of upper wave axis for disturbances passing 17° W.*

Distance ahead (n.mi.)	−240 to −120	−120 to 0	0 to +120	120 to 240	240 to 360	360 to 480	480 to 600
Number of cases	4	3	5	9	7	2	1

vection of relatively warm air (high thickness) from the vicinity of the Saharan heat low which would necessarily occur in the northeasterly flow ahead of the wave axis. Indeed, a comparison of two soundings made at station B, one on September 28 at a time of relatively low sea-level pressure and the other on October 1 when the pressure was high, shows that most of the pressure deficit could be accounted for by the presence of substantially warmer air between 700 mb and the surface on the day of lower pressure. The air was also much less humid in this layer and the flow was northeasterly, as compared to southeasterly on October 1. The axis of the sea-level pressure trough was found ahead of the upper wave axis in most cases, according to table 3.

In contrast to the soundings made in the relatively dry part of the system near 20° N., the data consistently show that in the vicinity of 15° N. the wave disturbances are relatively warm in the high troposphere and cold near the ground, with the strongest geopotential variations across the wave axis occurring near 600 mb. This is in agreement with the findings of paper I and the results of Simpson and others (1969). To this extent, and to the extent that the wave axis tends to slope eastward with height in the lower troposphere, the disturbances resemble the classical easterly wave of Riehl (1954). On the other hand, the symmetrical distribution of cloudiness in figure 4 is in contrast to the findings of paper I which showed a maximum of disturbed weather just ahead of the trough axis.

Another noteworthy aspect of figure 4 is a weak vortex located in the vicinity of the disturbance axis near 12° N. Examples of this type of vortex feature are found in figures 1 and 2. Figure 4 also illustrates that the greatest longitudinal variation in cloud cover across the wave axis (a change from 10 percent in the environment to 25 percent in the wave axis) is found between the latitudes of about 11° and 15° N. where, according to the results of paper I, the greatest instability and most intense convection are located. (Farther south, the clouds are mainly a dense and highly persistent stratocumulus.) The moist cloud-associated nature of this weak vortex is self evident in the analyses and suggests an origin and energy source related to the convective processes. In figure 2C, the weak vortex centered at 13° N. on the eastern side of disturbance 9/27 may have produced the minor fluctuation of the sea-level pressure (shown in fig. 3C) which followed the primary pressure oscillations at stations C and F. The same situation occurred with the subsequent disturbances 10/1. Interestingly, these minor wriggles in the pressure field were not observed at station A, which experienced a single strong pressure oscillation prior to the passage of the disturbance.

As can be seen in figure 1, the weak southern vortex associated with disturbance 9/11 is readily tracked over the ocean, while the northern center appears to vanish at the coastline or remain over land. Although this was characteristic for most disturbances, figure 3B shows that the pressure variations at Sal in the Cape Verde Islands (station Z) were as large as at Dakar (station D), suggesting that the low-level vorticity field associated with the disturbances continues to propagate over the ocean. It may be that the two vortexes merged together, although this could not be determined. Most probably, the southern vortex is identically that type of feature followed by Aspliden, Dean, and Landers (1966), who have tracked trains of surface vortices across the ocean from an apparent origin at the African coast between 10° and 15° N. The coordinates listed in column five of table 1 are the longitudes at which these vortexes first became recognizable in the analyses, and the latitudes of the centers.

In many instances, the aforementioned vortex was associated with a circular cloud area with noticeable spiral bands. Examples appear in disturbances 9/11 (fig. 1B) and 7/23 (fig. 2A). The appearance of such a cloud pattern is listed in column six of table 1 according to the longitude where it first became recognizable and the latitude of its apparent center. Merritt (1964) and Frank and Johnson (1969) both discuss the significance of vortical cloud patterns associated with weak tropical disturbances. Although many disturbances were very often associated with scanty amounts of cloud cover or poorly defined cloud systems well inland, the majority of waves developed a recognizable and coherent cloud structure (though not necessarily a circular one) and a vortex at 2,000 ft south of 15° N. prior to reaching the coast. Listed in column six of table 1 is the initially observed position (and latitude) of the circular cloud system.

According to paper I, the amount and degree of convective instability generally increases westward from the central portion of the West African bulge, creating an increasingly favorable environment for intensification after the disturbance reaches about 5° W. Although the disturbances appeared to achieve their greatest intensity in the area between 10° and 20° W. and sometime thereafter suffered a disintegration and disorganization of the cloud pattern, it was not difficult to follow prominent features of the cloud pattern over the ocean (see Frank, 1969). Accordingly, the date at which the disturbance reached the Antilles (60° W.), the speed in crossing the Atlantic Ocean and the date and longitude at which the wave was last observed were determined from satellite and wind data; and the information is listed in columns 7, 8, and 9, respectively, of table 1. Additional comments are made in column 10. These include the longitude at which the cloud pattern appeared to weaken over the ocean, another highly subjective evaluation but one which was derived from notes made concurrently with the events themselves.

TABLE 4.—*Frequency distribution of initial wave positions versus longitude*

Longitude interval	West of 4° E.	4° E. to 6° E.	7° E. to 9° E.	10° E. to 12° E.	13° E. to 15° E.	16° E. to 18° E.	East of data network
Number of fixes	4	2	1	6	3	2	14

Some of the disturbances appeared to be centered distinctly farther south than usual. These were labeled as "low latitude" disturbances in column five of table 1, although they are merely a variant of the type of system portrayed in the schematic diagram of figure 4A.

Table 4 contains a summary of the information contained in column 2 of table 1 according to the frequency of initial sightings versus intervals of longitude. According to the table, almost one-half of the disturbances appeared to originate east of the data network (18° E.), while only a few were first observed west of longitude 4° E. A minor peak exists in the interval between 10° and 12° E., suggesting a possible site favorable for wave initiation over the Cameroon Mountains. The generating mechanism over Africa may be, therefore, associated with an interaction of the convective processes with the terrain. If so, other mountainous sources would exist to the east of the data network over the Sudan and Ethiopia.

3. THE STATE OF AFRICAN DISTURBANCES OVER THE CARIBBEAN

The vast majority of the African disturbances in 1968 began to weaken west of the Cape Verde Islands, while only two hurricanes of marginal intensity developed from African disturbances. Visible on the satellite photographs was an increasing disintegration and disorganization of the cloud pattern followed by a collapse of the apparent cloud structure of the disturbance (Simpson and others, 1969); the weakening over the mid-Atlantic proved to be irreversible in almost all cases during 1968. As indicated in column 10 of table 1, the most rapid disintegration may have begun near 35° W.

Despite the visible weakening of the disturbances, the rainfall data (fig. 5) for St. Thomas (Virgin Islands) and Barbados (Windward Islands), two islands in the Antilles where a representative areal coverage of rain gages exists (seven for the former island and four on Barbados, the latter being available for only 2 mo in 1968), shows that there were a number of instances of wave passage over the particular island which corresponded closely to isolated peaks in the daily rainfall there. In order to present this observation in a statistical framework, a set of 5-day means centered on the day of wave passage by the island, as indicated by the arrows in figure 5, were determined for each disturbance to reach the island. The ratios of daily-to-mean rainfall for each of 5 days were composited for all cases where the data are available to form a normalized rainfall distribution. These results are shown in table 5.

Both stations display a mutually similar and systematic variation in rainfall during the period, in which the precipitation amount rises to a value substantially greater than normal on the day prior to wave passage and then falls to about one-half of the average daily rainfall on the day after wave passage. The table clearly implies that the disturbances retain a sufficient vertical-motion field over the Antilles to contribute significantly to the precipitation of these islands, although the contribution was occasionally little more than the heightening of the local island convection.

Also shown in figure 5 are the pressure fluctuations at longitudes 17° W. and 60° W., as indicated by the pair of digits listed above the box appropriate to that disturbance. The first figure corresponds to the pressure fluctuation at 17° W., as shown in column 4 of table 1 (rounded to the nearest whole millibar). The second figure, separated from the first by a dash, represents the corresponding sea-level fluctuation over the Antilles for that disturbance, as measured in a similar network of stations there. Comparison shows that the rises and falls in sea-level pressure over the Antilles were generally very much less than those over Africa, irrespective of the wave's initial intensity and organization. There is very little apparent relationship between either the magnitude of the sea-level pressure fluctuation or the degree of organization of the disturbance over Africa and the effects of the disturbance on the rainfall of the Antilles.

4. THE LARGE-SCALE WIND FIELD AND WAVE SPEED

The large-scale wind field over Africa in the belt of disturbances is characterized by southwesterly winds at low levels and strong easterlies aloft which are a consequence of the strong meridional temperature gradient between desert and ocean. In July, the northernmost penetration of the moist air is near 20° N., but as the systems shift southward in August and September (mirroring their northward advance during the spring), so does the confluence between the moist and dry regimes and the zone of convection. At the same time the desert air mass cools while the waters of the cross-equatorial flow in the Gulf of Guinea *warm*. The result is a weakening in the strength of the upper easterlies which is followed by a radical equatorward shift of the convective activity beginning in September or October.

The decrease in the mean easterly component of the atmosphere in the disturbance belt and the equatorward shift in the easterlies, which is especially pronounced over the African Continent, is illustrated by the graph of vertically integrated easterly flow in figure 6A.[1] According to figure 6B, there was a steady decrease in the phase speed of the waves from about 19 to 11 kt between July and

[1] The mean vertically averaged zonal wind refers to the 950- to 150-mb layer. The data comes from the U.S. Weather Bureau (Crutcher, 1961).

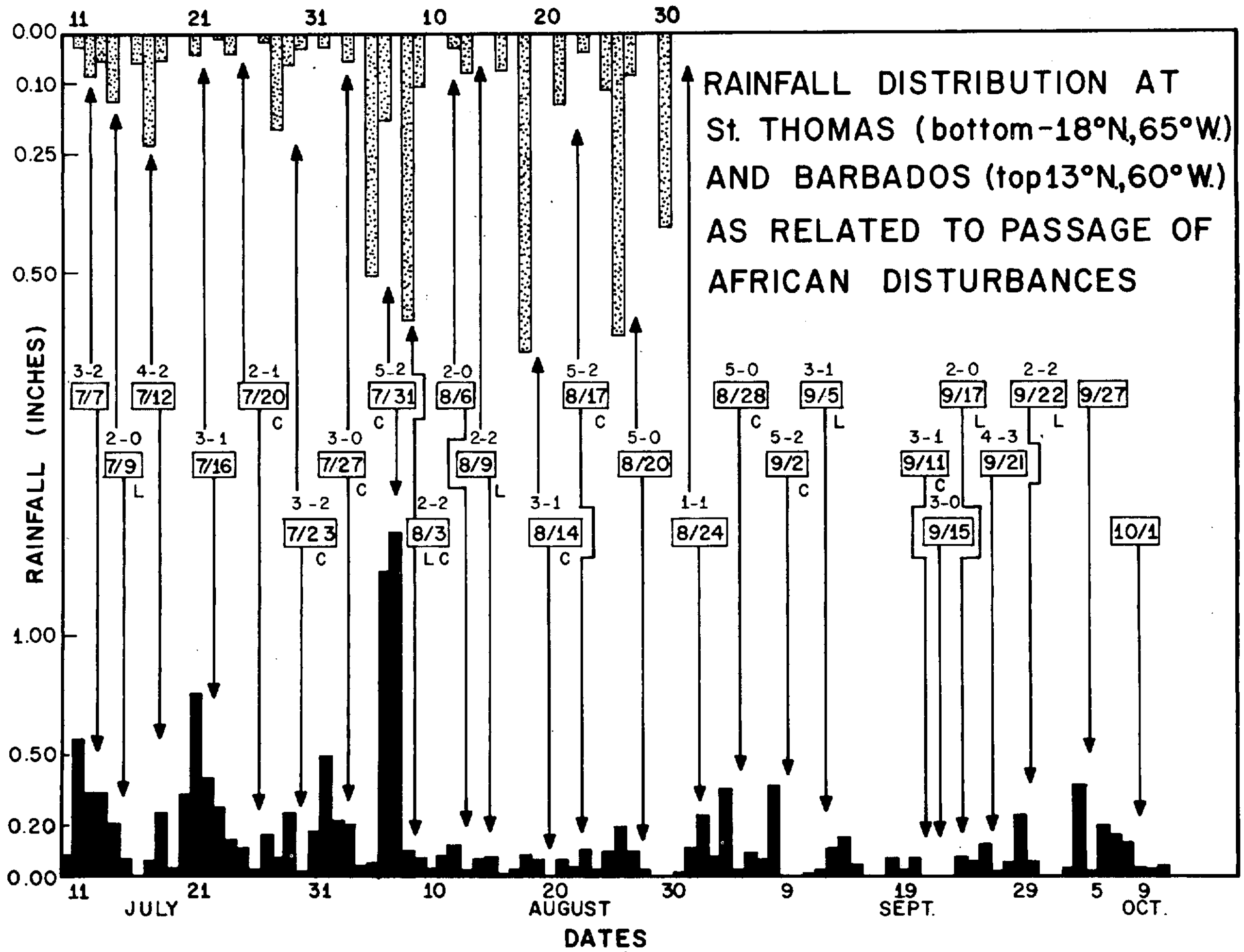

FIGURE 5.—Distribution of average daily rainfall at St. Thomas (bottom: average of seven stations) and Barbados (top: average of four stations), as related to the passage of African disturbances over the island (arrows labeled in boxes). The two digits at the top of the box (separated by a dash) are the sea-level pressure fluctuations (in millibars) for the disturbance when it was at the coast of Africa at 17° W. (left figure) and over the Antilles (right figure). The letter C, located just below the box, refers to systems that displayed a circular cloud pattern with attendant low-level vortex over Africa; the letter L refers to those systems that were observed to be at a lower latitude than usual (see table 1).

TABLE 5.—*Five-day normalized rainfall totals for African disturbances with respect to the day of passage by station (presented as fraction of average daily rainfall)*

Station	Number of cases	2 days earlier	1 day earlier	Day of passage	1 day later	2 days later	Average daily rainfall (inches)
(7 stations) St. Thomas	21	1.02	1.69	0.89	0.41	1.00	0.19
(4 stations) Barbados	14	0.81	1.19	1.02	0.60	1.38	0.10

October, which undoubtedly reflects the slowing of the large-scale easterly flow, shown in figure 6A.

Figure 6C is a plot of the average wave speed versus longitude. Although variations in speeds of less than a knot are considered statistically insignificant, the figure does show that the disturbances moved somewhat less rapidly over the continent than over the ocean (a fact which is readily apparent upon comparison of the values of the overall wave speed in column three with those in column nine of table 1). The point at which the disturbances began to accelerate (22° W.) corresponds to the axis of a large-scale upper trough (see fig. 7) which exists as a semipermanent feature along the entire coastline of the Euro-African landmass (U.S. Weather Bureau, 1952). Its presence is related to the geography and is necessitated by the removal and poleward transport of warm air from the continent. The corresponding ridge is found to coincide with the speed maximum at 45° W. By implication, the speed of disturbances is affected by the presence of large-scale trough and ridge patterns; in the mean they decelerate in the difluent (southeasterly) flow east of a trough and accelerate in the confluent (northeasterly) flow to the west of a trough, as is indicated by the segmented arrows in figure 6C. This is to be expected in a quasi-barotropic

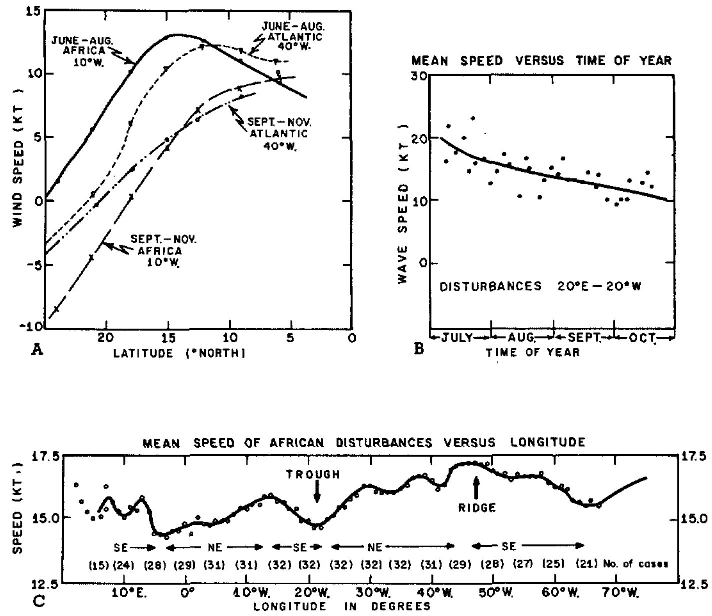

FIGURE 6.—(A) mean vertically averaged easterly wind profile between 150 and 950 mb versus latitude over Africa (10° W.) and over the mid-Atlantic (40° W.) for two periods of 3-mo averages centered on July and October; (B) seasonal distribution of wave speed over Africa for 1968; (C) composite distribution of wave speed versus longitude, averaged over the total number of cases indicated in parentheses. The arrow segments suggest intervals of southeasterly (SE) and northeasterly (NE) winds. The mean positions of major upper trough and ridge areas are also indicated.

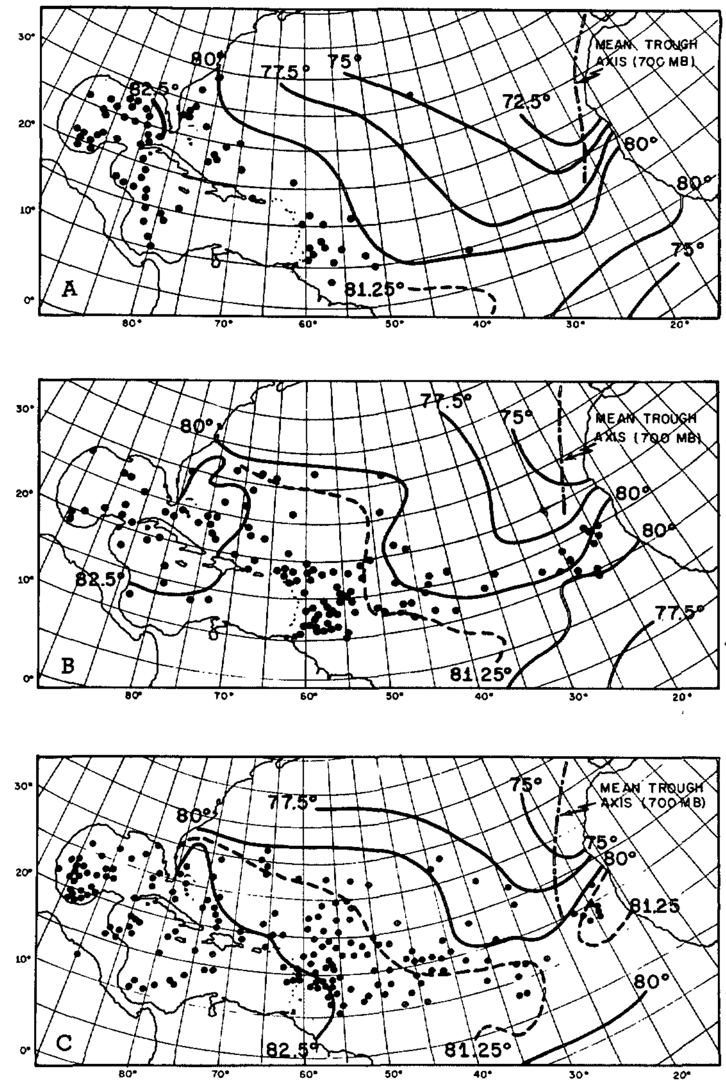

FIGURE 7.—Mean sea surface isotherms (°F), the distribution of initial tropical storm fixes, 1901–1967 (filled circles), and the mean position of the 700-mb wave axis for (A) June and July, (B) August, and (C) September.

current provided that the disturbances move with the mean (vertically integrated) speed of the flow. Interestingly, the areas favorable for large-scale ascent, the southeasterly regimes, are also those areas favorable for disturbance intensification, and vice versa with respect to northeasterly winds and disturbance dissipation. Certainly the strong northeasterly trades which exist from the longitude of the Cape Verde Islands westward are associated with cloud suppression.

5. THE INFLUENCE OF SEA-SURFACE TEMPERATURE

In addition to the dynamical factors in the suppression and enhancement of disturbances are the effects of sea-surface temperature. Closely linked to the geography and to the large-scale flow pattern, the strong northeasterly ocean current conveys cold water equatorward along the west coast of Africa to form a pronounced trough of cold water, shown in figures 7A–C,[2] which is located approximately between longitudes 25° and 45° W. Figures 7A–C illustrate the effects on tropical storm *formation* of the cold trough in the sea-surface temperature fields; in particular, the sensitivity of formation to the location of the 80°F (26.7°C) isotherm can be noted. The range of temperatures from 78°–82°F (26°–27°C) is generally accepted as being adequate for deepening of tropical disturbances from the depression stage through coupling of its convective processes and circulation with the oceanic energy source.

According to paper I, the distribution of convective instability over West Africa, as measured by the wet-bulb potential temperature at cloud base, θ_{wb}, is strongly influenced by the temperature of the ocean surface over which the trajectories of the low-level flow are originating. Figure 8 attempts to illustrate a relationship between sea-surface temperature and convective instability as it exists over the eastern tropical Atlantic during the summer months. It contains a plot of θ_{wb} (as computed for the 950-mb level but derived entirely from deck-level observations made onboard several research vessels in the tropical eastern Atlantic during the summer of 1963 and based on

[2] The sea temperatures in figures 7A–C are based upon values by Mazeika (1968) and upon those by the U.S. Hydrographic Office (1944). The tropical storm positions are updated to 1967 by the U.S. Weather Bureau (1965).

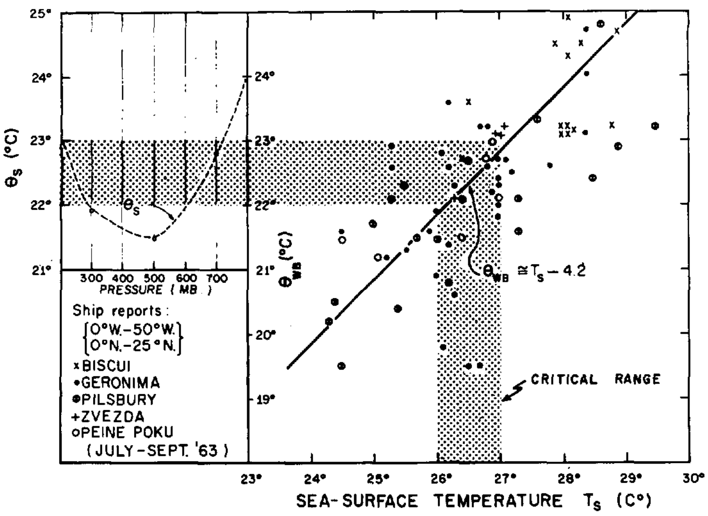

FIGURE 8.—Distribution of wet-bulb potential temperature at cloud base (θ_{wb}) and the sea-surface temperature (T_s) for the eastern tropical Atlantic during summertime. (Surface data were obtained from the five research ships identified at the lower left.) The straight line represents a visual fit to the scatter of points. At the upper left is the mean summertime saturation wet-bulb potential temperature (θ_s) versus pressure (in millibars) over the eastern tropical Atlantic. The shaded region signifies that sea-surface temperatures of 26° to 27°C are comparable to a θ_{wb} of 22° to 23°C which is barely sufficient to exceed θ_s in the middle and upper troposphere and thereby permit deep cumulonimbus convection.

lapse rates of potential temperature, adiabatic, and dew point, 0.5°C/10 mb, near the surface) versus sea-surface temperature, T_s. The cigar-shaped scatter of points suggests a straight line through its major axis having the analytical relationship $\theta_{wb} \approx T_s - 4.2$.

Since a variation in θ_{wb} of 1°C is equivalent to a change of 2.5°C in the temperature of a parcel ascending moist adiabatically into the high troposphere, it seems reasonable to assume that the convective instability (and hence the existence of the cumulonimbi) is closely controlled by the sea-surface temperature and its modification of the subcloud layer. Furthermore, when the value of θ_{wb}, as given by a particular sea-surface temperature in figure 8, is read against the scale of saturation wet-bulb potential temperature, θ_s (the temperature at a given pressure as measured on the scale of the moist adiabats), at the left of the diagram the former begins to exceed the mean value of θ_s in the middle and upper troposphere [3] (22°–23°C) where the temperature of the sea surface begins to exceed 26°–27°C (shaded region). At these latitudes deep convection, in which air parcels can reach the high troposphere, will therefore tend to be suppressed over water much cooler than about 80°F (26.7°C), even in the presence of large-scale ascending motion. Conversely, the growth of cumulonimbi is favored over water warmer than 80°F, provided that large-scale convergence is present in the lower layers.

[3] The mean sounding is a 3-yr average for three stations in the tropical Atlantic, Sal, Dakar, and Teneriffe, for the months of July through September during 1965–1967.

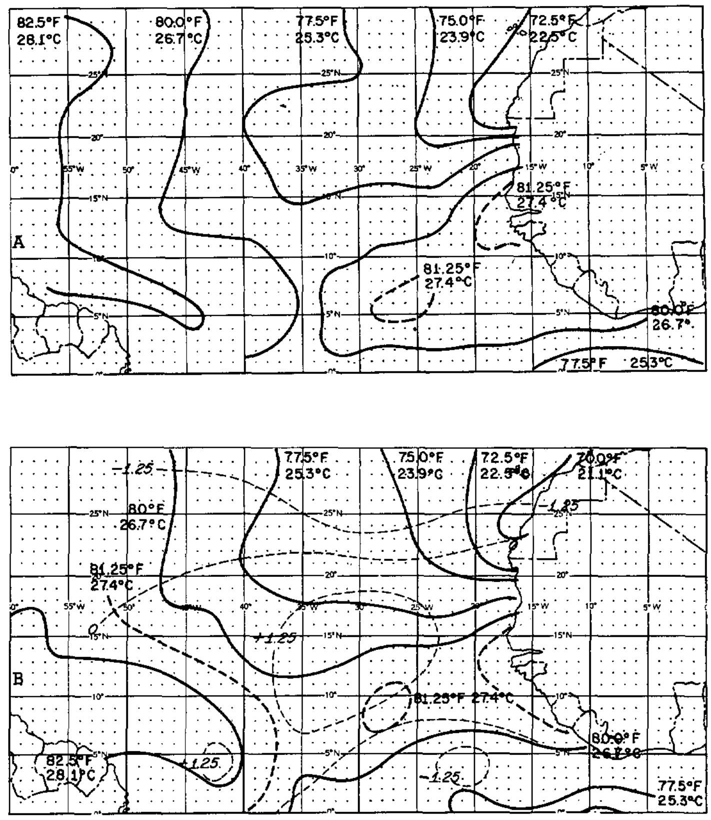

FIGURE 9.—Mean sea surface temperature field (in °C and °F) for (A) August 1968 and (B) August 1966. Also included in (B) is the departure isotherm field (dashed lines labeled in °F) of August 1966 from August 1968.

Figures 7A–C show that the 80°F isotherm extends south of 10° N. in early July but advances to a position a little north of 15° N. in September. Disturbances reaching 25° W. experience large-scale descent and an influx of stable air at low levels for a period of 3 to 5 days as they move westward. This normally hostile environment for disturbances mitigates as the season progresses. While only a very few disturbances are allowed to intensify in any year, the difference in tropical storm activity over the tropical Atlantic between seasons with abnormally cold and warm sea-surface temperatures may be highly significant as far as the total number of developing systems is concerned. This is particularly likely if the intrusion of cold sea temperatures and the strength of the upper trough are correlated positively.

Figure 9 shows the mean sea surface isotherms for August of 1968 and 1966. These fields were composited by the U.S. Fleet Numercial Weather Facility, Monterey, Calif., from an average of about 60 twice-daily computerized temperature fields drawn from their automated analysis program. August of 1968 is demonstrably cooler than that of 1966, a situation that is significant in view of the fact that 1968 was a notably weak hurricane season while 1966 was the most recent year with an above-average hurricane activity in the tropical Atlantic. The greatest differences in sea-surface temperature between the 2 mo occurred in the latitudes of the disturbance belt between 25° and 45° W. and near the mean position of the 80°F isotherm in that area (maximum difference of 2°F at 15° N., 35° W.). On the other hand, the waters immediately to the south and west of the southern coast of West Africa were warmer in August of 1968 than in August of any of the preceding years, a situation which would favor a higher degree of convective activity over Africa in 1968.

6. CONCLUSION

This paper represents an attempt to illustrate some important aspects of African disturbances, based on a wide sample of analyses for 1968. It is evident that the disturbances are large-scale (synoptic) wave pertubations with considerable latitudinal extent that exist apart from the ITC region, although they extend into that area. They are apparently not formed near the African coast nor (for the most part) over West Africa; rather, the disturbances originate primarily east of the African bulge, possibly over mountainous terrain. African disturbances are not a singular occurrence but move in continuous wave trains off the African coast. Most of them survive to reach the Antilles, their numbers constituting a possible majority of the population of disturbances in the eastern Caribbean. African disturbances achieve their greatest intensity near the African coast where they encounter an abundant supply of moist, convectively unstable air in the presence of a favorable large-scale wind regime. Thereafter they customarily suffer a disintegration which causes most of the disturbances to become very weak by the time they reach the Antilles. The disintegration seems to be related to the long-wave pattern of cold sea-surface temperatures west of the Cape Verde Islands and to the stabilizing effects of large-scale descent west of an offshore trough.

ACKNOWLEDGMENTS

The author is indebted to various members of the National Hurricane Center in Miami, Fla., for their cooperation in making available the synoptic and satellite data. In addition, we would like to thank the U.S. Naval Fleet Numerical Weather Facility in Monterey, Calif., for furnishing us upon request the computerized mean sea temperature fields. Critical suggestions and comments were offered by Mr. Harry F. Hawkins and Dr. R. Cecil Gentry of the National Hurricane Research Laboratory. Mr. Robert L. Carrodus was very helpful in drafting the figures. This author would also like to thank his assistant for the summer, Mr. Brian Jarvinen, for his help in analyzing the data. Additional rainfall data for Barbados was provided by Mr. Russ De Souza of the Florida State University. Mrs. Judy Greene typed the manuscript.

REFERENCES

Arnold, J. E., "Easterly Wave Activity Over Africa and in the Atlantic With a Note on the Intertropical Convergence Zone During Early July 1961," *Satellite and Mesometeorology Research Project Research Paper* No. 65, Department of the Geophysical Sciences, University of Chicago, Dec. **1966**, 23 pp.

Aspliden, C. I., Dean, G. A., and Landers, H., "Satellite Study, Tropical North Atlantic, 1963: Part 1. Surface Wind Analyses, September 1–September 30," *Research Report* No. 66–2, Department of Meteorology, Florida State University, Tallahassee, Mar. **1966**, 13 pp. plus numerous charts.

Crutcher, H. L., "Meridional Cross-Sections, Upper Winds over the Northern Hemisphere," *Technical Paper* No. 41, U.S. Weather Bureau, Washington, D.C., **1961**, 307 pp.

Carlson, T. N., "Synoptic Histories of Three African Disturbances That Developed Into Atlantic Hurricanes," *Monthly Weather Review*, Vol. 97, No. 3, Mar. **1969**, pp. 256–276.

Erickson, C. O., "An Incipient Hurricane Near the West African Coast," *Monthly Weather Review*, Vol. 91, No. 2, Feb. **1963**, pp. 61–68.

Frank, N. L., "The 'Inverted V' Cloud Pattern—An Easterly Wave?," *Monthly Weather Review*, Vol. 97, No. 2, Feb. **1969**, pp. 130–140.

Frank, N. L., and Johnson, H. M., "Vortical Cloud Systems Over the Tropical Atlantic During the 1967 Hurricane Season," *Monthly Weather Review*, Vol. 97, No. 2, Feb. **1969**, pp. 124–129.

Mazeika, P., "Mean Monthly Sea Surface Temperatures and Zonal Anomalies of the Tropical Atlantic," *The Serial Atlas of the Marine Environment*, American Geographical Society of New York, **1968**, (see Folio 16).

Merritt, E. S., "Easterly Waves and Perturbations, a Reappraisal," *Journal of Applied Meteorology*, Vol. 3, No. 4, Aug. **1964**, pp. 367–382.

Riehl, H., *Tropical Meteorology*, McGraw-Hill Book Co., Inc., New York, **1954**, 392 pp.

Simpson, R. H., Frank, N., Shideler, D., and Johnson, H. M., "Atlantic Tropical Disturbances, 1967," *Monthly Weather Review*, Vol. 96, No. 4, Apr. **1968**, pp. 251–259.

Simpson, R. H., Frank, N., Shideler, D., and Johnson, H. M., "Atlantic Tropical Disturbances of 1968," *Monthly Weather Review*, Vol. 97, No. 3, Mar. **1969**, pp. 240–255.

U.S. Hydrographic Office, *World Atlas of Sea Surface Temperatures*, 2d Edition, H.O. No. 225, Washington, D.C., **1944**.

U.S. Weather Bureau, "Normal Weather Maps for the Northern Hemisphere," *Technical Paper* No. 21, Washington, D.C., **1952**, 74 pp.

U.S. Weather Bureau, "Tropical Cyclones of the North Atlantic Ocean," *Technical Paper* No. 55, Washington, D.C., **1965**, 148 pp.

[*Received March 18, 1969; revised April 21, 1969*]